

A Discontinuous Enrichment Method (DEM) for Advection-Dominated Fluid Problems

Irina Kalashnikova*

Ph.D. Candidate

Institute for Computational & Mathematical Engineering (iCME)

Farhat Research Group (FRG)

Stanford University

Sandia National Laboratories

Albuquerque, NM

Aerosciences Department Seminar

Monday, August 23, 2010

* Joint work with Prof. Charbel Farhat and Dr. Radek Tezaur (Department of Aeronautics & Astronautics, Stanford University).



Background

■ Education:

- Ph.D. Candidate, Institute for Computational & Mathematical Engineering, Farhat Research Group, **Stanford University**, Stanford, CA (expected 2011).
- B.A., M.A., Mathematics, **University of Pennsylvania**, Philadelphia, PA (May 2006).

Current Research Interests: { Numerical solution to PDEs
Mixed/hybrid FEMs
Reduced Order Modeling, CFD

- **Recent Relevant Work Experience:** Graduate Technical Intern, Aeronautics Department (Org. 1515), **Sandia National Laboratories**, Albuquerque, NM (June 2007 – present).
 - Reduced Order Modeling of Fluid/Structure Interaction (Mentor: Matthew F. Barone, Org. 6333)
 - Modeling of Transitional and Fully Turbulent Pressure Fluctuation Loading (Mentor: Lawrence J. DeChant, Org. 1515)



Outline

- 1 Motivation
- 2 Advection-Diffusion Equation
- 3 Discontinuous Enrichment Method (DEM)
- 4 Advection-Diffusion DEM
 - Enrichment Bases
 - Lagrange Multiplier Approximations
 - Element Design
 - Variable-Coefficient Problems
 - 3D Advection-Diffusion
- 5 Numerical Experiments
 - Homogeneous Boundary Layer Problem
 - Double Ramp Problem on an L -Shaped Domain
 - Inhomogeneous Rotating Field Problem on an L -shaped Domain
- 6 Summary



Outline

- 1 Motivation
- 2 Advection-Diffusion Equation
- 3 Discontinuous Enrichment Method (DEM)
- 4 Advection-Diffusion DEM
 - Enrichment Bases
 - Lagrange Multiplier Approximations
 - Element Design
 - Variable-Coefficient Problems
 - 3D Advection-Diffusion
- 5 Numerical Experiments
 - Homogeneous Boundary Layer Problem
 - Double Ramp Problem on an L -Shaped Domain
 - Inhomogeneous Rotating Field Problem on an L -shaped Domain
- 6 Summary



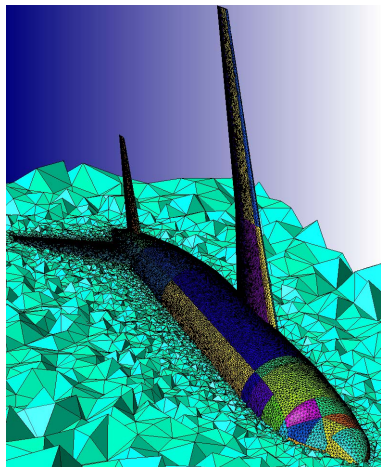
Outline

- 1 Motivation
- 2 Advection-Diffusion Equation
- 3 Discontinuous Enrichment Method (DEM)
- 4 Advection-Diffusion DEM
 - Enrichment Bases
 - Lagrange Multiplier Approximations
 - Element Design
 - Variable-Coefficient Problems
 - 3D Advection-Diffusion
- 5 Numerical Experiments
 - Homogeneous Boundary Layer Problem
 - Double Ramp Problem on an L -Shaped Domain
 - Inhomogeneous Rotating Field Problem on an L -shaped Domain
- 6 Summary



The Finite Element Method (FEM) in Fluid Mechanics

- Galerkin **Finite Element Method** (FEM) has a number of attractions in fluid mechanics:
 - Flexibility in handling complex geometries.
 - Ability to handle different forms of boundary conditions.
- FEM is quasi-optimal optimal for elliptic (diffusion-dominated) PDEs.

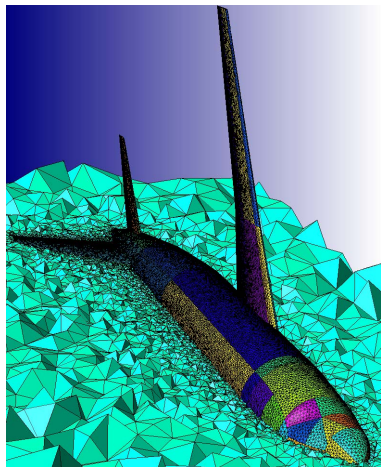


The Finite Element Method (FEM) in Fluid Mechanics

- Galerkin **Finite Element Method** (FEM) has a number of attractions in fluid mechanics:
 - Flexibility in handling complex geometries.
 - Ability to handle different forms of boundary conditions.
- FEM is quasi-optimal optimal for elliptic (diffusion-dominated) PDEs.

However:

FEM can yield “unstable” solutions when flow is advection-dominated



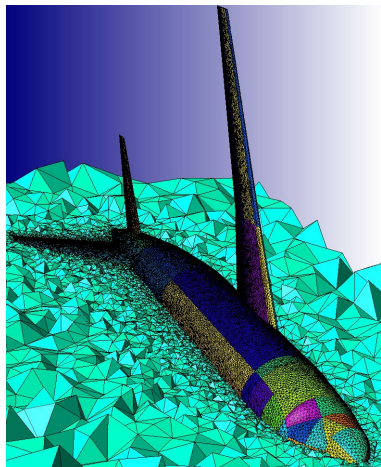
The Finite Element Method (FEM) in Fluid Mechanics

- Galerkin **Finite Element Method** (FEM) has a number of attractions in fluid mechanics:
 - Flexibility in handling complex geometries.
 - Ability to handle different forms of boundary conditions.
- FEM is quasi-optimal optimal for elliptic (diffusion-dominated) PDEs.

However:

FEM can yield “unstable” solutions when flow is advection-dominated

Significant mesh refinement typically needed to capture boundary layer region



The Finite Element Method (FEM) in Fluid Mechanics

- Galerkin **Finite Element Method** (FEM) has a number of attractions in fluid mechanics:
 - Flexibility in handling complex geometries.
 - Ability to handle different forms of boundary conditions.
- FEM is quasi-optimal optimal for elliptic (diffusion-dominated) PDEs.

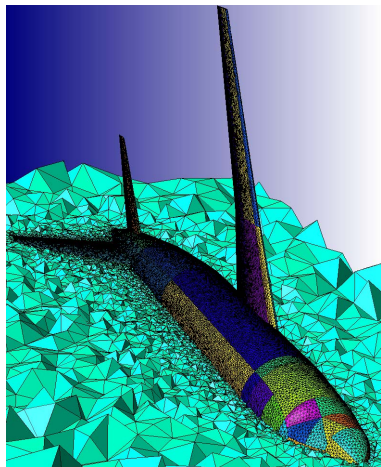
However:

FEM can yield “unstable” solutions when flow is advection-dominated

Significant mesh refinement typically needed to capture boundary layer region

EXPENSIVE!

- **Goal:** build an efficient method that can accurately capture boundary layers
- **Approach:** start with simple canonical problem; then generalize.



Outline

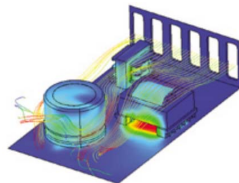
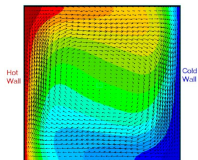
- 1 Motivation
- 2 Advection-Diffusion Equation
- 3 Discontinuous Enrichment Method (DEM)
- 4 Advection-Diffusion DEM
 - Enrichment Bases
 - Lagrange Multiplier Approximations
 - Element Design
 - Variable-Coefficient Problems
 - 3D Advection-Diffusion
- 5 Numerical Experiments
 - Homogeneous Boundary Layer Problem
 - Double Ramp Problem on an L -Shaped Domain
 - Inhomogeneous Rotating Field Problem on an L -shaped Domain
- 6 Summary



2D Scalar Advection-Diffusion Equation

$$\mathcal{L}u = \underbrace{-\kappa\Delta u}_{\text{diffusion}} + \underbrace{\mathbf{a} \cdot \nabla u}_{\text{advection}} = f$$

- Advection velocity:
 $\mathbf{a} = (a_1, a_2)^T = |\mathbf{a}|(\cos \phi, \sin \phi)^T$.
- ϕ = advection direction.
- κ = diffusivity.



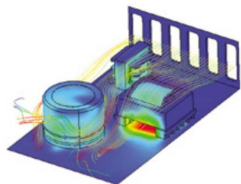
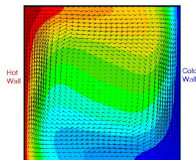
- Describes many transport phenomena in fluid mechanics:
 - Heat transfer.
 - Semiconductor device modeling.
 - Usual scalar model for the more challenging Navier-Stokes equations.



2D Scalar Advection-Diffusion Equation

$$\mathcal{L}u = \underbrace{-\kappa\Delta u}_{\text{diffusion}} + \underbrace{\mathbf{a} \cdot \nabla u}_{\text{advection}} = f$$

- Advection velocity:
 $\mathbf{a} = (a_1, a_2)^T = |\mathbf{a}|(\cos \phi, \sin \phi)^T$.
- ϕ = advection direction.
- κ = diffusivity.



- Describes many transport phenomena in fluid mechanics:
 - Heat transfer.
 - Semiconductor device modeling.
 - Usual scalar model for the more challenging Navier-Stokes equations.
- Global **Péclet number** (L = length scale associated with Ω):

$$Pe = \frac{\text{rate of advection}}{\text{rate of diffusion}} = \frac{L|\mathbf{a}|}{\kappa} = Re \cdot \begin{cases} Pr & \text{(thermal diffusion)} \\ Sc & \text{(mass diffusion)} \end{cases}$$



Advection-Dominated Regime

- Typical applications: flow is advection dominated.

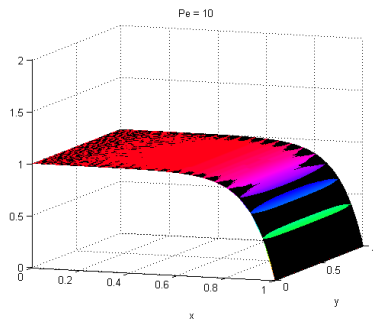


Figure 1: Galerkin Q_1 solution (color) vs. exact solution (black) as $Pe \uparrow$ ($Pe = 10 \rightarrow 150$)

Advection-Dominated
(High Pe) Regime
 \Downarrow
 Sharp gradients in exact solution
 \Downarrow
 Galerkin FEM inadequate:
 spurious oscillations (Fig. 1)

- Some classical remedies:
 - **Stabilized FEMs** (SUPG, GLS, USFEM): add weighted residual (numerical diffusion) to variational equation.
 - **RFB, VMS, PUM**: construct conforming spaces that incorporate knowledge of local behavior of solution.



Advection-Dominated Regime

- Typical applications: flow is advection dominated.

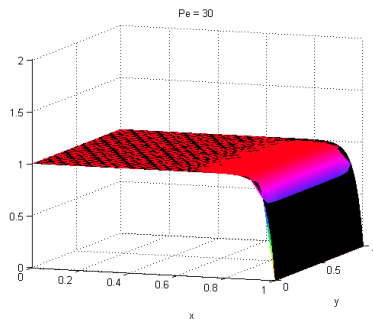


Figure 1: Galerkin Q_1 solution (color) vs. exact solution (black) as $Pe \uparrow$ ($Pe = 10 \rightarrow 150$)

Advection-Dominated
(High Pe) Regime
 \Downarrow
 Sharp gradients in exact solution
 \Downarrow
 Galerkin FEM inadequate:
 spurious oscillations (Fig. 1)

- Some classical remedies:
 - **Stabilized FEMs** (SUPG, GLS, USFEM): add weighted residual (numerical diffusion) to variational equation.
 - **RFB, VMS, PUM**: construct conforming spaces that incorporate knowledge of local behavior of solution.



Advection-Dominated Regime

- Typical applications: flow is advection dominated.

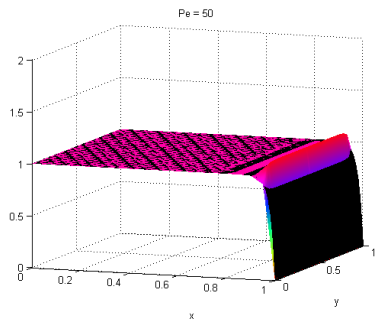


Figure 1: Galerkin Q_1 solution (color) vs. exact solution (black) as $Pe \uparrow$ ($Pe = 10 \rightarrow 150$)

Advection-Dominated
(High Pe) Regime
 \Downarrow
 Sharp gradients in exact solution
 \Downarrow
 Galerkin FEM inadequate:
 spurious oscillations (Fig. 1)

- Some classical remedies:
 - **Stabilized FEMs** (SUPG, GLS, USFEM): add weighted residual (numerical diffusion) to variational equation.
 - **RFB, VMS, PUM**: construct conforming spaces that incorporate knowledge of local behavior of solution.



Advection-Dominated Regime

- Typical applications: flow is advection dominated.

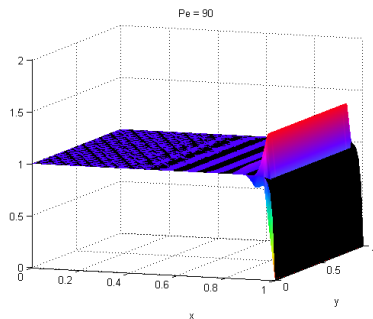


Figure 1: Galerkin Q_1 solution (color) vs. exact solution (black) as $Pe \uparrow$ ($Pe = 10 \rightarrow 150$)

Advection-Dominated
(High Pe) Regime
 \Downarrow
 Sharp gradients in exact solution
 \Downarrow
 Galerkin FEM inadequate:
 spurious oscillations (Fig. 1)

- Some classical remedies:
 - **Stabilized FEMs** (SUPG, GLS, USFEM): add weighted residual (numerical diffusion) to variational equation.
 - **RFB, VMS, PUM**: construct conforming spaces that incorporate knowledge of local behavior of solution.



Advection-Dominated Regime

- Typical applications: flow is advection dominated.

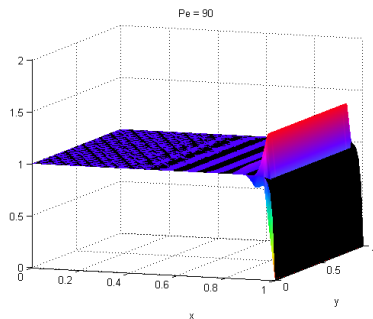


Figure 1: Galerkin Q_1 solution (color) vs. exact solution (black) as $Pe \uparrow$ ($Pe = 10 \rightarrow 150$)

Advection-Dominated
(High Pe) Regime
 \Downarrow
 Sharp gradients in exact solution
 \Downarrow
 Galerkin FEM inadequate:
 spurious oscillations (Fig. 1)

- Some classical remedies:
 - **Stabilized FEMs** (SUPG, GLS, USFEM): add weighted residual (numerical diffusion) to variational equation.
 - **RFB, VMS, PUM**: construct conforming spaces that incorporate knowledge of local behavior of solution.



Advection-Dominated Regime

- Typical applications: flow is advection dominated.

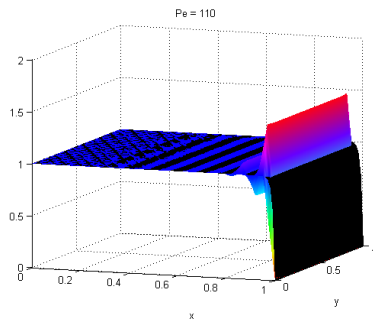


Figure 1: Galerkin Q_1 solution (color) vs. exact solution (black) as $Pe \uparrow$ ($Pe = 10 \rightarrow 150$)

Advection-Dominated
(High Pe) Regime
 \Downarrow
 Sharp gradients in exact solution
 \Downarrow
 Galerkin FEM inadequate:
 spurious oscillations (Fig. 1)

- Some classical remedies:
 - **Stabilized FEMs** (SUPG, GLS, USFEM): add weighted residual (numerical diffusion) to variational equation.
 - **RFB, VMS, PUM**: construct conforming spaces that incorporate knowledge of local behavior of solution.



Advection-Dominated Regime

- Typical applications: flow is advection dominated.

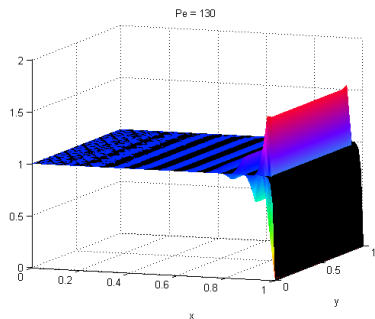


Figure 1: Galerkin Q_1 solution (color) vs. exact solution (black) as $Pe \uparrow$ ($Pe = 10 \rightarrow 150$)

Advection-Dominated
(High Pe) Regime
 \Downarrow
 Sharp gradients in exact solution
 \Downarrow
 Galerkin FEM inadequate:
 spurious oscillations (Fig. 1)

- Some classical remedies:
 - **Stabilized FEMs** (SUPG, GLS, USFEM): add weighted residual (numerical diffusion) to variational equation.
 - **RFB, VMS, PUM**: construct conforming spaces that incorporate knowledge of local behavior of solution.



Advection-Dominated Regime

- Typical applications: flow is advection dominated.

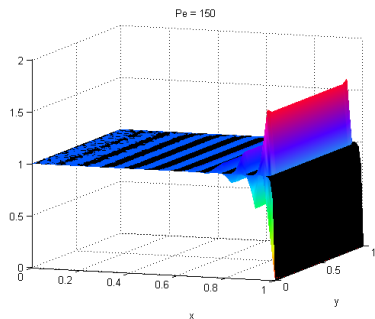


Figure 1: Galerkin Q_1 solution (color) vs. exact solution (black) as $Pe \uparrow$ ($Pe = 10 \rightarrow 150$)

Advection-Dominated
(High Pe) Regime
 \Downarrow
 Sharp gradients in exact solution
 \Downarrow
 Galerkin FEM inadequate:
 spurious oscillations (Fig. 1)

- Some classical remedies:
 - **Stabilized FEMs** (SUPG, GLS, USFEM): add weighted residual (numerical diffusion) to variational equation.
 - **RFB, VMS, PUM**: construct conforming spaces that incorporate knowledge of local behavior of solution.



Outline

- 1 Motivation
- 2 Advection-Diffusion Equation
- 3 Discontinuous Enrichment Method (DEM)
- 4 Advection-Diffusion DEM
 - Enrichment Bases
 - Lagrange Multiplier Approximations
 - Element Design
 - Variable-Coefficient Problems
 - 3D Advection-Diffusion
- 5 Numerical Experiments
 - Homogeneous Boundary Layer Problem
 - Double Ramp Problem on an L -Shaped Domain
 - Inhomogeneous Rotating Field Problem on an L -shaped Domain
- 6 Summary



The Discontinuous Enrichment Method (DEM)

- First developed by Farhat *et. al.* in 2000 for the Helmholtz equation.

Idea of DEM:

“Enrich” the usual Galerkin polynomial field \mathcal{V}^P by the free-space solutions to the governing homogeneous PDE $\mathcal{L}u = 0$.

$$u^h = u^P + u^E \in \mathcal{V}^P \oplus (\mathcal{V}^E \setminus \mathcal{V}^P)$$

where

$$\mathcal{V}^E = \text{span}\{u : \mathcal{L}u = 0\}$$

- Simple 1D Example:**

$$\begin{cases} u_x - u_{xx} = 1 + x, & x \in (0, 1) \\ u(0) = 0, u(1) = 1 \end{cases}$$

- Enrichments:** $u_x^E - u_{xx}^E = 0 \Rightarrow u^E = C_1 + C_2 e^x \Rightarrow \mathcal{V}^E = \text{span}\{1, e^x\}$

- Galerkin FEM polynomials:** $\mathcal{V}_{\Omega^e=(x_j, x_{j+1})}^P = \text{span}\left\{\frac{x_{j+1}-x}{h}, \frac{x-x_j}{h}\right\}$



Two Variants of DEM

- Two variants of DEM: “pure DGM” vs. “true DEM”

	DGM	DEM
\mathcal{V}^h	\mathcal{V}^E	$\mathcal{V}^P \oplus (\mathcal{V}^E \setminus \mathcal{V}^P)$
u^h	u^E	$u^P + u^E$

Enrichment-Only “Pure DGM”:

Contribution of the standard polynomial field is dropped entirely from the approximation.

Genuine or “Full” DEM:

Splitting of the approximation into coarse (polynomial) and fine (enrichment) scales.

- Unlike PUM, VMS & RFB: enrichment field in DEM is not required to vanish at element boundaries



Two Variants of DEM

- Two variants of DEM: “pure DGM” vs. “true DEM”

	DGM	DEM
\mathcal{V}^h	\mathcal{V}^E	$\mathcal{V}^P \oplus (\mathcal{V}^E \setminus \mathcal{V}^P)$
u^h	u^E	$u^P + u^E$

Enrichment-Only “Pure DGM”:

Contribution of the standard polynomial field is dropped entirely from the approximation.

Genuine or “Full” DEM:

Splitting of the approximation into coarse (polynomial) and fine (enrichment) scales.

- Unlike PUM, VMS & RFB: enrichment field in DEM is not required to vanish at element boundaries \Rightarrow DEM is **discontinuous** by construction!

DEM = DGM with Lagrange Multipliers



What about Inter-Element Continuity?

- Continuity across element boundaries is enforced weakly using Lagrange multipliers $\lambda^h \in \mathcal{W}^h$:

$$\lambda^h \approx \nabla u_e^E \cdot \mathbf{n}^e = -\nabla u_{e'}^E \cdot \mathbf{n}^{e'} \quad \text{on } \Gamma^{e,e'}$$

but making sure we uphold the...

- Discrete **Babuška-Brezzi *inf-sup* condition**¹:

$$\left\{ \begin{array}{l} \# \text{ Lagrange multiplier} \\ \text{constraint equations} \end{array} \leq \begin{array}{l} \# \text{ enrichment} \\ \text{equations} \end{array} \right\}$$

Rule of thumb to satisfy the Babuška-Brezzi *inf-sup* condition is to limit:

$$n^\lambda = \left\lfloor \frac{n^E}{4} \right\rfloor \equiv \max \left\{ n \in \mathbb{Z} \mid n \leq \frac{n^E}{4} \right\}$$

$$\begin{aligned} n^\lambda &= \# \text{ Lagrange multipliers per edge} \\ n^E &= \# \text{ enrichment functions} \end{aligned}$$

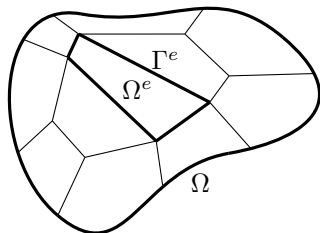
¹Necessary condition for generating a non-singular global discrete problem. 



Hybrid Variational Formulation of DEM

■ Strong form:

$$(S) : \begin{cases} \text{Find } u \in H^1(\Omega) \text{ such that} \\ -\kappa \Delta u + \mathbf{a} \cdot \nabla u = f, & \text{in } \Omega \\ u = g, & \text{on } \Gamma = \partial\Omega \\ u_e - u_{e'} = 0 & \text{on } \Gamma^{\text{int}} \end{cases}$$



■ Weak hybrid variational form:

$$(W) : \begin{cases} \text{Find } (u, \lambda) \in \mathcal{V} \times \mathcal{W} \text{ such that:} \\ a(v, u) + b(\lambda, v) = r(v) \\ b(\mu, u) = -r_d(\mu) \\ \text{holds } \forall v \in \mathcal{V}, \forall \mu \in \mathcal{W}. \end{cases}$$

where

$$a(v, u) = (\kappa \nabla v + v \mathbf{a}, \nabla u)_{\tilde{\Omega}}$$

$$b(\lambda, v) = \sum_e \sum_{e' < e} \int_{\Gamma^{e,e'}} \lambda (v_{e'} - v_e) d\Gamma + \int_{\Gamma} \lambda v d\Gamma$$

Notation:

$$\tilde{\Omega} = \cup_{e=1}^{n_{el}} \Omega^e$$

$$\tilde{\Gamma} = \cup_{e=1}^{n_{el}} \Gamma^e$$

$$\Gamma^{e,e'} = \Gamma^e \cap \Gamma^{e'}$$

$$\Gamma^{\text{int}} = \cup_{e' < e} \cup_{e=1}^{n_{el}} \{\Gamma^e \cap \Gamma^{e'}\}$$



Discretization & Implementation

- Element matrix problem (uncondensed):

$$\begin{pmatrix} \mathbf{k}^{PP} & \mathbf{k}^{PE} & \mathbf{k}^{PC} \\ \mathbf{k}^{EP} & \mathbf{k}^{EE} & \mathbf{k}^{EC} \\ \mathbf{k}^{CP} & \mathbf{k}^{CE} & \mathbf{0} \end{pmatrix} \begin{pmatrix} \mathbf{u}^P \\ \mathbf{u}^E \\ \lambda^h \end{pmatrix} = \begin{pmatrix} \mathbf{r}^P \\ \mathbf{r}^E \\ \mathbf{r}^C \end{pmatrix}$$



Discretization & Implementation

- Element matrix problem (uncondensed):

$$\begin{pmatrix} \mathbf{k}^{PP} & \mathbf{k}^{PE} & \mathbf{k}^{PC} \\ \mathbf{k}^{EP} & \mathbf{k}^{EE} & \mathbf{k}^{EC} \\ \mathbf{k}^{CP} & \mathbf{k}^{CE} & \mathbf{0} \end{pmatrix} \begin{pmatrix} \mathbf{u}^P \\ \mathbf{u}^E \\ \lambda^h \end{pmatrix} = \begin{pmatrix} \mathbf{r}^P \\ \mathbf{r}^E \\ \mathbf{r}^C \end{pmatrix}$$

Due to the discontinuous nature of \mathcal{V}^E , \mathbf{u}^E can be eliminated at the element level by a static condensation



Discretization & Implementation

- Element matrix problem (uncondensed):

$$\begin{pmatrix} \mathbf{k}^{PP} & \mathbf{k}^{PE} & \mathbf{k}^{PC} \\ \mathbf{k}^{EP} & \mathbf{k}^{EE} & \mathbf{k}^{EC} \\ \mathbf{k}^{CP} & \mathbf{k}^{CE} & \mathbf{0} \end{pmatrix} \begin{pmatrix} \mathbf{u}^P \\ \mathbf{u}^E \\ \lambda^h \end{pmatrix} = \begin{pmatrix} \mathbf{r}^P \\ \mathbf{r}^E \\ \mathbf{r}^C \end{pmatrix}$$

Due to the discontinuous nature of \mathcal{V}^E , \mathbf{u}^E can be eliminated at the element level by a static condensation

- Statically-condensed **True DEM Element**:

$$\begin{pmatrix} \tilde{\mathbf{k}}^{PP} & \tilde{\mathbf{k}}^{PC} \\ \tilde{\mathbf{k}}^{CP} & \tilde{\mathbf{k}}^{CC} \end{pmatrix} \begin{pmatrix} \mathbf{u}^P \\ \lambda^h \end{pmatrix} = \begin{pmatrix} \tilde{\mathbf{r}}^P \\ \tilde{\mathbf{r}}^C \end{pmatrix}$$

- Statically-condensed **Pure DGM Element**:

$$-\mathbf{k}^{CE}(\mathbf{k}^{EE})^{-1}\mathbf{k}^{EC}\lambda^h = \mathbf{r}^C - \mathbf{k}^{CE}(\mathbf{k}^{EE})^{-1}\mathbf{r}^E,$$



Discretization & Implementation

- Element matrix problem (uncondensed):

$$\begin{pmatrix} \mathbf{k}^{PP} & \mathbf{k}^{PE} & \mathbf{k}^{PC} \\ \mathbf{k}^{EP} & \mathbf{k}^{EE} & \mathbf{k}^{EC} \\ \mathbf{k}^{CP} & \mathbf{k}^{CE} & \mathbf{0} \end{pmatrix} \begin{pmatrix} \mathbf{u}^P \\ \mathbf{u}^E \\ \lambda^h \end{pmatrix} = \begin{pmatrix} \mathbf{r}^P \\ \mathbf{r}^E \\ \mathbf{r}^C \end{pmatrix}$$

Computational complexity depends on $\dim \mathcal{V}^h$ not on $\dim \mathcal{V}^E$

Due to the discontinuous nature of \mathcal{V}^E , \mathbf{u}^E can be eliminated at the element level by a static condensation

- Statically-condensed **True DEM Element**:

$$\begin{pmatrix} \tilde{\mathbf{k}}^{PP} & \tilde{\mathbf{k}}^{PC} \\ \tilde{\mathbf{k}}^{CP} & \tilde{\mathbf{k}}^{CC} \end{pmatrix} \begin{pmatrix} \mathbf{u}^P \\ \lambda^h \end{pmatrix} = \begin{pmatrix} \tilde{\mathbf{r}}^P \\ \tilde{\mathbf{r}}^C \end{pmatrix}$$

- Statically-condensed **Pure DGM Element**:

$$-\mathbf{k}^{CE} (\mathbf{k}^{EE})^{-1} \mathbf{k}^{EC} \lambda^h = \mathbf{r}^C - \mathbf{k}^{CE} (\mathbf{k}^{EE})^{-1} \mathbf{r}^E,$$



Outline

- 1 Motivation
- 2 Advection-Diffusion Equation
- 3 Discontinuous Enrichment Method (DEM)
- 4 Advection-Diffusion DEM**
 - Enrichment Bases
 - Lagrange Multiplier Approximations
 - Element Design
 - Variable-Coefficient Problems
 - 3D Advection-Diffusion
- 5 Numerical Experiments
 - Homogeneous Boundary Layer Problem
 - Double Ramp Problem on an L -Shaped Domain
 - Inhomogeneous Rotating Field Problem on an L -shaped Domain
- 6 Summary



Angle-Parametrized Enrichment Functions for 2D Advection-Diffusion

- Derived by solving $\mathcal{L}u^E = \mathbf{a} \cdot \nabla u^E - \kappa \Delta u^E = 0$ analytically (e.g., separation of variables).

$$u^E(\mathbf{x}; \theta_i) = e^{\left(\frac{a_1 + |\mathbf{a}| \cos \theta_i}{2\kappa}\right)(x - x_{r,i})} e^{\left(\frac{a_2 + |\mathbf{a}| \sin \theta_i}{2\kappa}\right)(y - y_{r,i})} \quad (1)$$

$\Theta^u \equiv \{\theta_i\}_{i=1}^{n^E} \in [0, 2\pi) =$ set of angles specifying \mathcal{V}^E

$(x_{r,i}, y_{r,i}) =$ reference point for u_i^E

$\mathbf{a}^T \equiv (a_1, a_2) =$ advection velocity vector

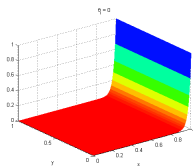
The parametrization with respect to θ_i in (1) is non-trivial!

- Enrichment functions are now specified by a set of “flow directions”.
- Without this parametrization, systematic element design would not be possible!

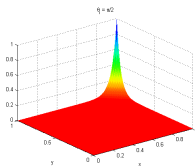


Plots of Enrichment Functions for Some Angles

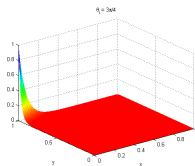
$$\theta_i \in [0, 2\pi)$$



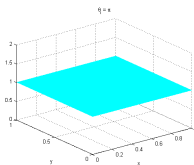
$$\phi = 0, \theta_i = 0$$



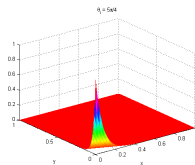
$$\phi = 0, \theta_i = \frac{\pi}{2}$$



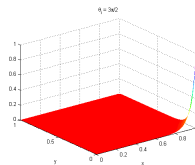
$$\phi = \frac{\pi}{2}, \theta_i = \frac{3\pi}{4}$$



$$\phi = 0, \theta_i = \pi$$



$$\phi = \frac{3\pi}{2}, \theta_i = \frac{5\pi}{4}$$



$$\phi = 0, \theta_i = \frac{3\pi}{2}$$

Figure 2: Plots of enrichment function $u^E(\mathbf{x}; \theta_i)$ for several values of θ_i ($Pe = 20$)



What about the Lagrange Multiplier Approximations?

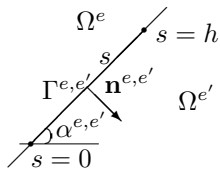


Figure 3: Straight edge $\Gamma^{e,e'}$ oriented at angle $\alpha^{e,e'} \in [0, 2\pi)$

- Trivial to compute given exponential enrichments:

$$\begin{aligned} \lambda^h(s)|_{\Gamma^{e,e'}} &\approx \nabla u^E \cdot \mathbf{n}|_{\Gamma^{e,e'}} \\ &= C \cdot e^{\left\{ \frac{|\mathbf{a}|}{2\kappa} [\cos(\phi - \alpha^{e,e'}) + \cos(\theta_k - \alpha^{e,e'})] (s - s_r^{e,e'}) \right\}} \end{aligned}$$



What about the Lagrange Multiplier Approximations?

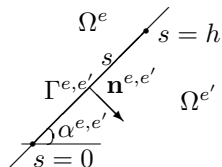


Figure 3: Straight edge $\Gamma^{e,e'}$ oriented at angle $\alpha^{e,e'} \in [0, 2\pi)$

- Trivial to compute given exponential enrichments:

$$\begin{aligned} \lambda^h(s)|_{\Gamma^{e,e'}} &\approx \nabla u^E \cdot \mathbf{n}|_{\Gamma^{e,e'}} \\ &= C \cdot e^{\left\{ \frac{|\mathbf{a}|}{2\kappa} [\cos(\phi - \alpha^{e,e'}) + \cos(\theta_k - \alpha^{e,e'})] (s - s_r^{e,e'}) \right\}} \end{aligned}$$

Non-trivial to satisfy *inf-sup* condition:
the set Θ^u that defines \mathcal{V}^E typically leads to
too many Lagrange multiplier dofs!



Lagrange Multiplier Selection

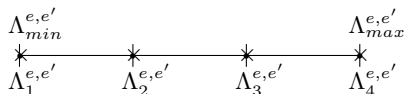


Illustration of Lagrange Multiplier selection for $n^\lambda = 4$

- Define:

$$\Lambda_i^{e,e'} \equiv \frac{|\mathbf{a}|}{2\kappa} \left[\cos(\phi - \alpha^{e,e'}) + \cos(\theta_k - \alpha^{e,e'}) \right]$$

↓

$$\lambda^h|_{\Gamma^{e,e'}} = \text{span} \left\{ e^{\Lambda_i^{e,e'}(s-s_{r,i}^{e,e'})}, 0 \leq s \leq h \right\}$$

- Determine # Lagrange multipliers allowed: $\text{card}\{\Lambda_i^{e,e'}\} = \left\lfloor \frac{n^E}{4} \right\rfloor$.
- Sample $\Lambda_i^{e,e'}$ uniformly in the interval $[\Lambda_{min}^{e,e'}, \Lambda_{max}^{e,e'}]$ to span space of all exponentials of the form $\{e^{\Lambda_i^{e,e'}s} : \Lambda_{min}^{e,e'} \leq \Lambda_i^{e,e'} \leq \Lambda_{max}^{e,e'}\}$.



Mesh Independent Element Design Procedure

Algorithm 1. "Build your own DEM element"

Fix $n^E \in \mathbb{N}$ (the desired number of angles defining \mathcal{V}^E).

Select a set of n^E distinct angles $\{\theta_k\}_{k=1}^{n^E}$ between $[0, 2\pi)$.

Let $\Theta^u = \phi + \{\theta_i\}_{i=1}^{n^E}$.

Define the enrichment functions by:

$$u^E(\mathbf{x}; \Theta^u) = e^{\left(\frac{a_1 + |\mathbf{a}| \cos \Theta^u}{2\kappa}\right)(x - x_{r,i})} e^{\left(\frac{a_2 + |\mathbf{a}| \sin \Theta^u}{2\kappa}\right)(y - y_{r,i})}$$

Determine $n^\lambda = \lfloor \frac{n^E}{4} \rfloor$.

for each edge $\Gamma^{e,e'} \in \Gamma^{\text{int}}$

Compute max and min of $\frac{|\mathbf{a}|}{2\kappa} [\cos(\phi - \alpha^{e,e'}) + \cos(\theta_k - \alpha^{e,e'})]$, call them $\Lambda_{\min}^{e,e'}$, $\Lambda_{\max}^{e,e'}$.

Sample $\{\Lambda_i^{e,e'} : i = 1, \dots, n^\lambda\}$ uniformly in the interval $[\Lambda_{\min}^{e,e'}, \Lambda_{\max}^{e,e'}]$.

Define the Lagrange multipliers approximations on $\Gamma^{e,e'}$ by:

$$\lambda^h|_{\Gamma^{e,e'}} = \text{span} \left\{ e^{\Lambda_i^{e,e'}(s - s_{r,i}^{e,e'})}, 0 \leq s \leq h \right\}$$

end for



Some DGM/DEM Elements

Notation

DGM Element: $Q - n^E - n^\lambda$

DEM Element: $Q - n^E - n^{\lambda+} \equiv [Q - n^E - n^\lambda] \cup [Q_1]$

'Q': Quadrilateral

n^E : Number of Enrichment Functions

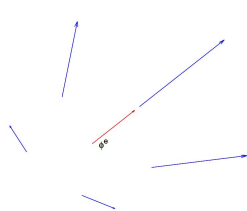
n^λ : Number of Lagrange Multipliers per Edge

Q_1 : Galerkin Bilinear Quadrilateral Element

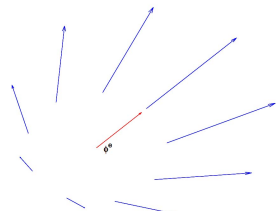
	Name	n^E	Θ^u	n^λ
DGM elements	$Q - 4 - 1$	4	$\phi + \left\{ \frac{m\pi}{2} : m = 0, \dots, 3 \right\}$	1
	$Q - 8 - 2$	8	$\phi + \left\{ \frac{m\pi}{4} : m = 0, \dots, 7 \right\}$	2
	$Q - 12 - 3$	12	$\phi + \left\{ \frac{m\pi}{6} : m = 0, \dots, 11 \right\}$	3
	$Q - 16 - 4$	16	$\phi + \left\{ \frac{m\pi}{8} : m = 0, \dots, 15 \right\}$	4
DEM elements	$Q - 5 - 1^+$	5	$\phi + \left\{ \frac{2m\pi}{5} : m = 0, \dots, 4 \right\}$	1
	$Q - 9 - 2^+$	9	$\phi + \left\{ \frac{2m\pi}{9} : m = 0, \dots, 8 \right\}$	2
	$Q - 13 - 3^+$	13	$\phi + \left\{ \frac{2m\pi}{13} : m = 0, \dots, 12 \right\}$	3
	$Q - 17 - 4^+$	17	$\phi + \left\{ \frac{2m\pi}{17} : m = 0, \dots, 16 \right\}$	4



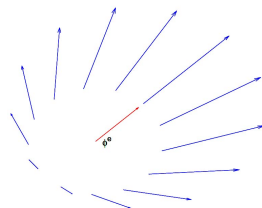
Illustration of the Sets Θ^u for the True DEM Elements



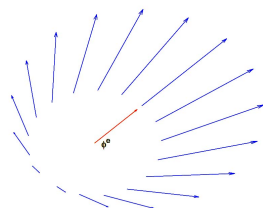
$Q-5-1^+$



$Q-9-2^+$



$Q-13-3^+$



$Q-17-4^+$



Computational Properties

Element	Asymptotic # of dofs	Stencil width for uniform $n \times n$ mesh
Q_1	n_{el}	9
Q_2	$3n_{el}$	21
Q_3	$5n_{el}$	33
Q_4	$7n_{el}$	45
$Q - 4 - 1$	$2n_{el}$	7
$Q - 8 - 2$	$4n_{el}$	14
$Q - 12 - 3$	$6n_{el}$	21
$Q - 16 - 4$	$8n_{el}$	28
$Q - 5 - 1^+$	$3n_{el}$	21
$Q - 9 - 2^+$	$5n_{el}$	33
$Q - 13 - 3^+$	$7n_{el}$	45
$Q - 17 - 4^+$	$9n_{el}$	57

- Exponential enrichments \Rightarrow integrations computed analytically.
- $\mathcal{L}u^E = 0 \Rightarrow$ convert volume integrals to boundary integrals:

$$a(v^E, u^E) = \int_{\tilde{\Omega}} (\kappa \nabla v^E \cdot \nabla u^E + \mathbf{a} \cdot \nabla u^E v^E) d\Omega = \int_{\tilde{\Gamma}} \nabla u^E \cdot \mathbf{n} v^E d\Gamma.$$

Figure 4: Q_1 stencil

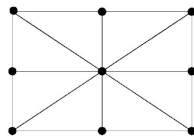
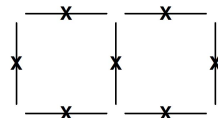
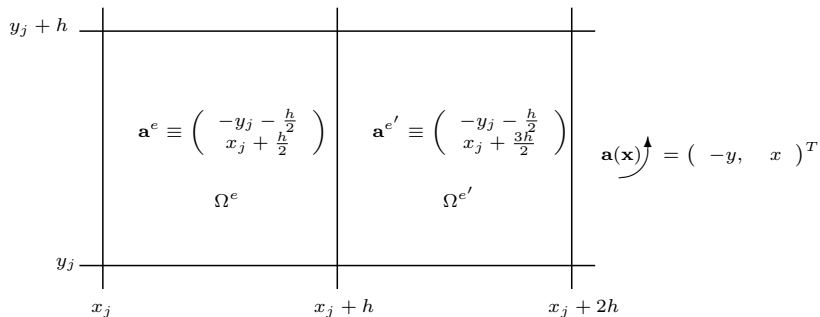


Figure 5: $Q - 4 - 1$ stencil



DEM for Variable-Coefficient Advection-Diffusion

- Define \mathcal{V}^E *within each element* as the free-space solutions to the homogeneous PDE, with locally-frozen coefficients.
 - $\mathbf{a}(\mathbf{x}) \approx \mathbf{a}^e = \text{constant}$ inside each element Ω^e as $h \rightarrow 0$:
- $$\{\mathbf{a}(\mathbf{x}) \cdot \nabla u - \kappa \Delta u = f(\mathbf{x}) \text{ in } \Omega\} \approx \cup_e^{nel} \{\mathbf{a}^e \cdot \nabla u - \kappa \Delta u = f(\mathbf{x}) \text{ in } \Omega^e\}$$



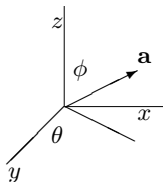
- Enrichment in each element:

$$u_e^E(\mathbf{x}; \theta_i^e) = e^{\frac{|\mathbf{a}^e|}{2\kappa} (\cos \phi^e + \cos \theta_i^e)(x - x_{r,i}^e)} e^{\frac{|\mathbf{a}^e|}{2\kappa} (\sin \phi^e + \sin \theta_i^e)(y - y_{r,i}^e)} \in \mathcal{V}_e^E$$



Extension to 3D Advection-Diffusion

- Advection direction: specified by two angles $(\theta, \phi) \in [0, 2\pi) \times [0, \pi)$



- Advection velocity vector: $\mathbf{a}^T = (\sin \phi \cos \theta, \sin \phi \sin \theta, \cos \phi)$
- Enrichment functions for 3D advection-diffusion:

$$u^E(\mathbf{x}; \phi_i, \theta_i) = e^{\frac{1}{2\kappa} [\sin \phi \cos \theta + \sin \phi_i \cos \theta_i] x} e^{\frac{1}{2\kappa} [\sin \phi \sin \theta + \sin \phi_i \sin \theta_i] y} e^{\frac{1}{2\kappa} [\cos \phi + \cos \phi_i] z}$$

$$\Phi \times \Theta \equiv \{(\theta_i, \phi_i)\}_{i=1}^{n^E} \in [0, 2\pi) \times [0, \pi) = \text{set of angles specifying } \mathcal{V}^E$$



Outline

- 1 Motivation
- 2 Advection-Diffusion Equation
- 3 Discontinuous Enrichment Method (DEM)
- 4 Advection-Diffusion DEM
 - Enrichment Bases
 - Lagrange Multiplier Approximations
 - Element Design
 - Variable-Coefficient Problems
 - 3D Advection-Diffusion
- 5 Numerical Experiments
 - Homogeneous Boundary Layer Problem
 - Double Ramp Problem on an L -Shaped Domain
 - Inhomogeneous Rotating Field Problem on an L -shaped Domain
- 6 Summary



Homogeneous Boundary Layer Problem

- $\Omega = (0, 1) \times (0, 1)$, $f = 0$.
- $\mathbf{a} = \begin{pmatrix} \cos \phi & \sin \phi \end{pmatrix}$.
- Dirichlet boundary conditions are specified on Γ such that the exact solution to the BVP is given by

$$u_{ex}(\mathbf{x}; \phi, \psi) = \frac{e^{\frac{1}{2\kappa} \{[\cos \phi + \cos \psi](x-1) + [\sin \phi + \sin \psi](y-1)\}} - 1}{e^{-\frac{1}{2\kappa} [\cos \phi + \cos \psi + \sin \phi + \sin \psi]} - 1}$$

- $\psi \in [0, 2\pi)$: some flow direction (not necessarily aligned with ϕ).
- Solution exhibits a sharp exponential boundary layer in the advection direction ϕ , whose gradient is a function of the Péclet number.

Figure 6: $\phi = \psi = 0$

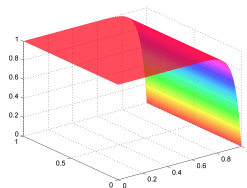
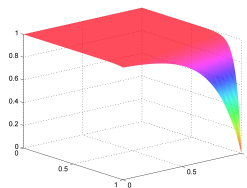


Figure 7: $\phi = \pi/7, \psi = 0$



Homogeneous Boundary Layer Problem

- $\Omega = (0, 1) \times (0, 1)$, $f = 0$.
- $\mathbf{a} = \begin{pmatrix} \cos \phi & \sin \phi \end{pmatrix}$.
- Dirichlet boundary conditions are specified on Γ such that the exact solution to the BVP is given by

$$u_{ex}(\mathbf{x}; \phi, \psi) = \frac{e^{\frac{1}{2\kappa} \{[\cos \phi + \cos \psi](x-1) + [\sin \phi + \sin \psi](y-1)\}} - 1}{e^{-\frac{1}{2\kappa} [\cos \phi + \cos \psi + \sin \phi + \sin \psi]} - 1}$$

- $\psi \in [0, 2\pi)$: some flow direction (not necessarily aligned with ϕ).
- Solution exhibits a sharp exponential boundary layer in the advection direction ϕ , whose gradient is a function of the Péclet number.

Homogeneous problem \Rightarrow
pure DGM elements sufficient

Figure 6: $\phi = \psi = 0$

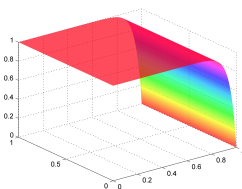
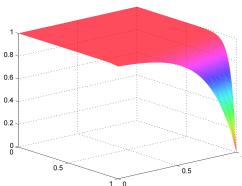


Figure 7: $\phi = \pi/7, \psi = 0$



Flow Aligned with Advection Direction ($\phi = \psi$)

- $u_{ex} \in \mathcal{V}^E$ for *all* DGM elements, for all advection directions ϕ here.



Flow Aligned with Advection Direction ($\phi = \psi$)

- $u_{ex} \in \mathcal{V}^E$ for *all* DGM elements, for all advection directions ϕ here.
- Therefore one would expect these elements to capture the exact solution to machine precision



Flow Aligned with Advection Direction ($\phi = \psi$)

- $u_{ex} \in \mathcal{V}^E$ for all DGM elements, for all advection directions ϕ here.
- Therefore one would expect these elements to capture the exact solution to machine precision – *but only provided* $\nabla u_{ex} \cdot \mathbf{n} \in \mathcal{W}^h$.

Table 1: Relative $L^2(\Omega)$ errors, ≈ 400 dofs, $Pe = 10^3$, uniform mesh: Galerkin vs. DGM elts.

ϕ/π	Q_1	$Q - 4 - 1$	Q_2	$Q - 8 - 2$
0	5.77×10^{-1}	3.43×10^{-14}	4.33×10^{-1}	2.22×10^{-10}
1/6	2.53×10^{-2}	1.24×10^{-15}	1.49×10^{-2}	8.38×10^{-4}
1/4	2.62×10^{-2}	3.19×10^{-14}	1.53×10^{-2}	5.62×10^{-6}
ϕ/π	Q_3	$Q - 12 - 3$	Q_4	$Q - 16 - 4$
0	3.68×10^{-1}	5.78×10^{-13}	2.44×10^{-1}	9.75×10^{-10}
1/6	1.21×10^{-2}	5.50×10^{-6}	9.47×10^{-3}	3.31×10^{-6}
1/4	1.24×10^{-2}	4.36×10^{-14}	9.81×10^{-3}	1.27×10^{-12}



Flow *not* Aligned with Advection Direction ($\phi \neq \psi$)

- Fix $\phi = \pi/7$, vary ψ .



Flow *not* Aligned with Advection Direction ($\phi \neq \psi$)

- Fix $\phi = \pi/7$, vary ψ .
- Can show that $u_{ex} \notin \mathcal{V}^E$ for any DGM elements and advection directions tested here.

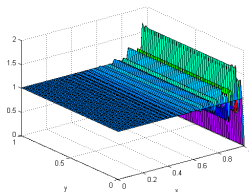
Table 2: Relative $L^2(\Omega)$ errors, ≈ 1600 dofs, unstructured mesh, $\phi = \pi/7$, $Pe = 10^3$: Galerkin vs. DGM elts.

ψ/π	Q_1	$Q - 4 - 1$	Q_2	$Q - 8 - 2$
0	1.45×10^{-2}	1.65×10^{-3}	5.92×10^{-3}	1.79×10^{-3}
1/4	1.52×10^{-2}	9.38×10^{-4}	6.06×10^{-3}	2.54×10^{-4}
1/2	1.51×10^{-2}	9.23×10^{-4}	5.97×10^{-3}	2.12×10^{-4}
ψ/π	Q_3	$Q - 12 - 3$	Q_4	$Q - 16 - 4$
0	4.34×10^{-3}	1.10×10^{-4}	3.23×10^{-3}	2.30×10^{-5}
1/4	4.46×10^{-3}	1.23×10^{-5}	3.29×10^{-3}	8.82×10^{-7}
1/2	4.36×10^{-3}	1.11×10^{-5}	3.18×10^{-3}	1.59×10^{-6}

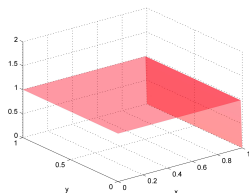


Solution Plots for Homogeneous BVP

Figure 8: $\phi = \psi = 0$, $Pe = 10^3$, ≈ 1600 dofs

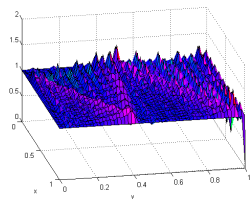


Q_3

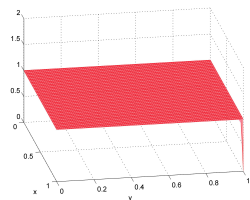


$Q - 12 - 3$

Figure 9: $\phi = \pi/7$, $\psi = 0$, $Pe = 10^5$, ≈ 1600 dofs



Q_3



$Q - 12 - 3$



Convergence Analysis

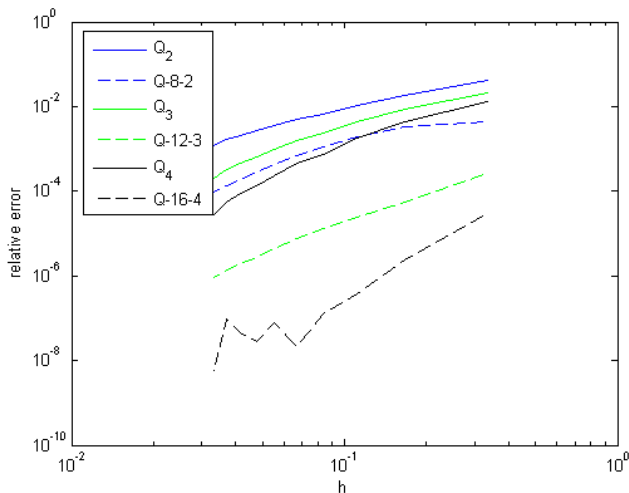
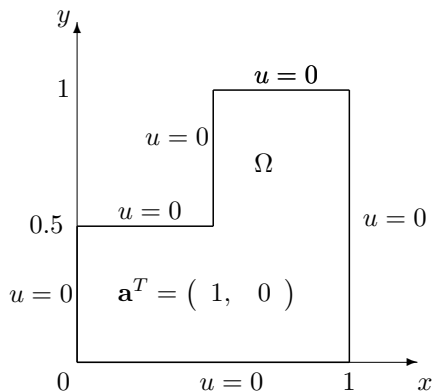


Figure 10: Convergence Rates ($\phi = \pi/7, \psi = 0, Pe = 10^2$, unstructured mesh)



Double Ramp Problem on an L -Shaped Domain



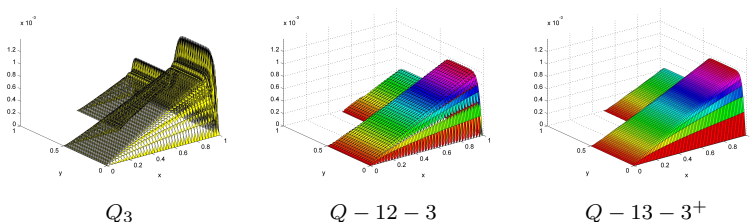
- Homogeneous Dirichlet boundary conditions are prescribed on all six sides of L -shaped domain Ω
- Advection direction: $\phi = 0$
- Source: $f = 1$
- Strong outflow boundary layer along the line $x = 1$
- Two crosswind boundary layers along $y = 0$ and $y = 1$
- A crosswind internal layer along $y = 0.5$

Figure 11: L -shaped domain for double ramp problem



Solutions Plots: Galerkin vs. DGM vs. DEM Elements

Figure 12: L-shaped double ramp problem solutions: $Pe = 10^3$, 7600 dofs

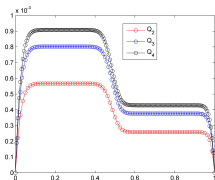


- No oscillations can be seen in the computed DGM and DEM solutions.
- Would expect: DEM elements to outperform DGM elements for this *inhomogeneous* problem.
- In fact: DGM elements experience some difficulty along the $y = 0.5$ line, the location of the crosswind internal layer.

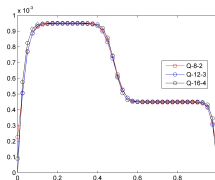


Cross Sectional Solution Plots

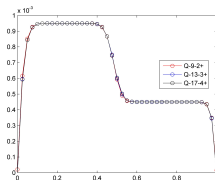
Figure 13: Solution along the line $x = 0.9$ with 7600 dofs



Galerkin

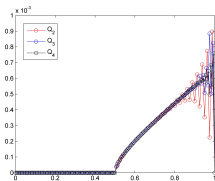


DGM

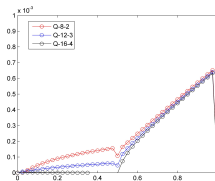


DEM

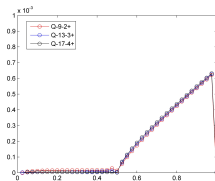
Figure 14: Solution along the line $y = 0.5$ with 7600 dofs



Galerkin



DGM



DEM



Relative Errors

Table 3: $L^2(\Omega)$ errors relative to a reference solution*: uniform mesh, $Pe = 10^3$

# dofs	Q_2	$Q - 8 - 2$	$Q - 9 - 2^+$
900	2.72×10^{-1}	1.19×10^{-1}	7.22×10^{-2}
3600	1.23×10^{-1}	6.07×10^{-2}	1.51×10^{-2}
14,400	5.26×10^{-2}	2.81×10^{-2}	3.10×10^{-3}
32,400	2.92×10^{-2}	1.54×10^{-2}	1.80×10^{-3}
# dofs	Q_3	$Q - 12 - 3$	$Q - 13 - 3^+$
1500	1.49×10^{-1}	1.11×10^{-1}	5.62×10^{-2}
6000	6.57×10^{-2}	5.00×10^{-2}	6.90×10^{-3}
24,000	2.36×10^{-2}	1.02×10^{-2}	8.45×10^{-4}
54,000	1.08×10^{-2}	4.54×10^{-3}	2.48×10^{-4}
# dofs	Q_4	$Q - 16 - 4$	$Q - 17 - 4^+$
2100	9.58×10^{-2}	8.32×10^{-2}	4.66×10^{-2}
8400	3.78×10^{-2}	1.33×10^{-2}	3.08×10^{-3}
33,600	1.03×10^{-2}	9.17×10^{-3}	2.04×10^{-4}
75,600	3.70×10^{-3}	4.92×10^{-4}	4.16×10^{-5}

- * Since an analytical solution to this problem is not available, in computing the relative error, we use in place of the exact solution a reference solution, computed using a Galerkin Q_6 polynomial element on a $43,200 = 3 \cdot (120 \times 120)$ element mesh.



Inhomogeneous Rotating Advection Problem on an L-Shaped Domain

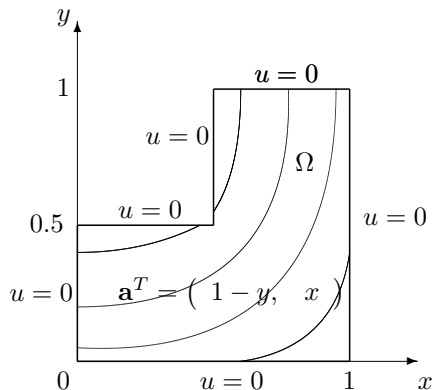
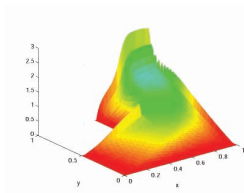
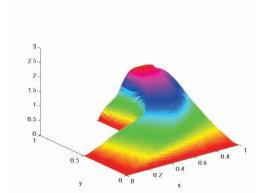
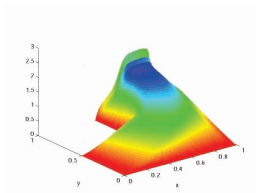
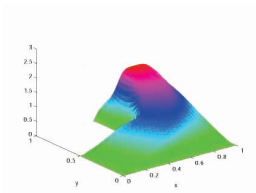
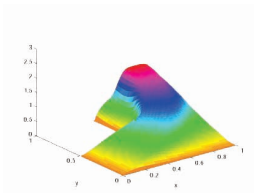


Figure 15: L-shaped domain and rotating velocity field (curved lines indicate streamlines)

- Homogeneous Dirichlet boundary conditions are prescribed on all six sides of L-shaped domain Ω
- $\mathbf{a}^T(\mathbf{x}) = \begin{pmatrix} 1 - y & x \end{pmatrix}$
- Source: $f = 1$
- Outflow boundary layer along the line $y = 1$
- Second boundary layer that terminates in the vicinity of the re-entrant corner $(x, y) = (0.5, 0.5)$.

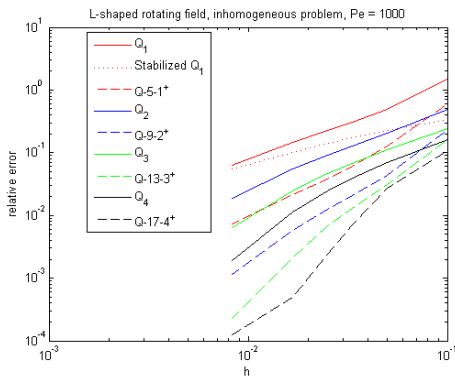


Solutions Plots for $Pe = 10^3$ with ≈ 3000 dofs Q_1 Stabilized Q_1  Q_2  $Q - 5 - 1^+$  $Q - 9 - 2^+$

* “Stabilized Q_1 ” is upwind stabilized bilinear finite element proposed by Harari *et al.*



Convergence Analysis & Results



- To achieve for this problem the relative error of 0.1%:
 - $Q-5-1^+$ requires 6.4 times fewer dofs than Q_1 .
 - $Q-9-2^+$ requires 8.3 times fewer dofs than Q_2 .
 - $Q-13-3^+$ requires 5.7 times fewer dofs than Q_3 .
 - $Q-17-4^+$ requires 4.3 times fewer dofs than Q_4 .

* “Stabilized Q_1 ” is upwind stabilized bilinear finite element proposed by Harari *et al.*



Outline

- 1 Motivation
- 2 Advection-Diffusion Equation
- 3 Discontinuous Enrichment Method (DEM)
- 4 Advection-Diffusion DEM
 - Enrichment Bases
 - Lagrange Multiplier Approximations
 - Element Design
 - Variable-Coefficient Problems
 - 3D Advection-Diffusion
- 5 Numerical Experiments
 - Homogeneous Boundary Layer Problem
 - Double Ramp Problem on an L -Shaped Domain
 - Inhomogeneous Rotating Field Problem on an L -shaped Domain
- 6 Summary



Summary

Discontinuous Enrichment Method (DEM) = efficient, competitive alternative to stabilized FEMs for advection diffusion in a high Péclet regime.

- Parametrization makes possible systematic design of DEM elements of arbitrary orders.
- For all test problems, the enriched elements outperform their Galerkin and stabilized Galerkin counterparts of comparable computational complexity by at least one (and sometimes many) orders of magnitude difference
- In a high Péclet regime, DGM and DEM solutions are almost completely oscillation-free, in contrast with the Galerkin solutions.
- Advection-diffusion work generalizable to more complex equations in fluid mechanics (e.g., 3D, non-linear, unsteady).
- Future work: projection-method based DEM for incompressible Navier Stokes.



Publications

(www.stanford.edu/~irinak/pubs.html)

DEM:

- [1] **I. Kalashnikova**, R. Tezaur, C. Farhat. A Discontinuous Enrichment Method for Variable Coefficient Advection-Diffusion at High Peclet Number. *Int. J. Numer. Meth. Engng.* (accepted)
- [2] C. Farhat, **I. Kalashnikova**, R. Tezaur. A Higher-Order Discontinuous Enrichment Method for the Solution of High Peclet Advection-Diffusion Problems on Unstructured Meshes. *Int. J. Numer. Meth. Engng.* **81** (2010) 604-636.
- [3] **I. Kalashnikova**, C. Farhat, R. Tezaur. A Discontinuous Enrichment Method for the Solution of Advection-Diffusion Problems in high Peclet Number Regimes. *Fin. El. Anal. Des.* **45** (2009) 238-250.

ROM:

- [4] M.F. Barone, **I. Kalashnikova**, M.R. Brake, D.J. Segalman. Reduced Order Modeling of Fluid/Structure Interaction. *Sandia National Laboratories Report, SAND No. 2009-7189*. Sandia National Laboratories, Albuquerque, NM (2010).
- [5] **I. Kalashnikova**, M.F. Barone. On the Stability and Convergence of a Galerkin Reduced Order Model (ROM) of Compressible Flow with Solid Wall and Far-Field Boundary Treatment. *Int. J. Numer. Meth. Engng.* (in press).
- [6] M.F. Barone, **I. Kalashnikova**, D.J. Segalman, H. Thornquist. Stable Galerkin Reduced Order Models for Linearized Compressible Flow. *J. Comput. Phys.* **288** (2009) 1932-1946.
- [7] M.F. Barone, D.J. Segalman, H. Thornquist, **I. Kalashnikova**. Galerkin Reduced Order Models for Compressible Flow with Structural Interaction. *AIAA Paper No. 2008-0612*, 46th AIAA Aerospace Science Meeting and Exhibit, Reno, NV (Jan. 2008).

